Biogeosciences Discuss., 9, 16663–16704, 2012
www.biogeosciences-discuss.net/9/16663/2012/
doi:10.5194/bgd-9-16663-2012
© Author(s) 2012. CC Attribution 3.0 License.

Biogeosciences Discussions

This discussion paper is/has been under review for the journal Biogeosciences (BG).
Please refer to the corresponding final paper in BG if available.

Lingulodinium machaerophorum expansion over the last centuries in the Caspian Sea reflects global warming

S. A. G. Leroy[1], H. A. K. Lahijani[2], J.-L. Reyss[3], F. Chalié[4], S. Haghani[1,2,5], M. Shah-Hosseini[2,4], S. Shahkarami[2,5], A. Tudryn[6], K. Arpe[1,7], P. Habibi[2], H. S. Nasrollahzadeh[8], and A. Makhlough[8]

[1]Institute for the Environment, Brunel University, Kingston Lane, Uxbridge UB8 3PH, West London, UK
[2]Iranian National Institute for Oceanography (INIO), No 3, Etemadzadeh St., Fatemi Av., Tehran 1411813389, Iran
[3]Laboratoire des Sciences du Climat et de l'Environnement, CEA-CNRS, Avenue de la Terrasse, 91198 Gif-sur-Yvette Cedex, France
[4]Aix-Marseille Université, CEREGE, UMR7330 CNRS, UM34, 13545 Aix-en-Provence cedex 04, France
[5]School of Geology, University of Tehran, Enghelab Sq., Tehran, Iran
[6]Laboratoire CNRS/UPS UMR 8148 IDES, Université de Paris XI, Département des Sciences de la Terre, Bâtiment 504, 91 405 ORSAY cedex, France
[7]Max Plank Institute for Meteorology, Hamburg, Germany
[8]Ecology Departments, Caspian Sea Ecology Research Center (CSERC), 961 Sari, Iran

Received: 8 October 2012 – Accepted: 12 November 2012 – Published: 22 November 2012

Correspondence to: S. A. G. Leroy (suzanne.leroy@brunel.ac.uk)

Published by Copernicus Publications on behalf of the European Geosciences Union.

BGD

9, 16663–16704, 2012

Abstract

We analysed dinoflagellate cyst assemblages in four short sediment cores, two of them dated by radionuclides, taken in the south basin of the Caspian Sea. The interpretation of the four sequences is supported by a collection of 27 lagoonal or marine surface sediment samples. A sharp increase in the biomass of the dinocyst occurs after 1967, especially owing to *Lingulodinium machaerophorum*. Considering nine other cores covering parts or the whole of Holocene, this species started to develop in the Caspian Sea only during the last three millennia. By analysing instrumental data and collating existing reconstructions of sea level changes over the last few millennia, we show that the main forcing of the increase of *L. machaerophorum* percentages and of the recent dinocyst abundance is global climate change, especially sea surface temperature increase. Sea level fluctuations likely have a minor impact. We argue that the Caspian Sea has entered the Anthropocene.

1 Introduction

The Caspian Sea (CS) is the largest inland water body in the world (Fig. 1). It is well known for the petroleum and caviar it produces. This unique ecosystem with many endemic species is under increasing pressure. The monitoring of its ecosystem changes is inconsistent across the five bordering countries, because of their different socio-economical level; so an accurate overview of the environmental changes affecting ecosystem processes at present is not available. The instrumental records of the last century indicate rapid changes in sea surface temperature, in sea level and in trophic levels. Sea level changes are large, close to 3 m amplitude and a hundred times faster than that of the global ocean in the 20th century (Crétaux and Birkett, 2006; Fig. 2a), but also as much as 20 m amplitude in the last few millennia (Kakroodi et al., 2012). The sea surface temperature of the south basin especially in the summer shows a warming trend over the last century (Ginzburg et al., 2005).

BGD
9, 16663–16704, 2012

The use of dinocyst-inferred reconstruction of past water parameters, such as temperature, salinity, and nutrient levels, is a powerful palaeoenvironmental approach that may contribute to understanding many of the problems listed above (Marret and Zonneveld, 2003). So far however very few dinocyst analyses are available for recent times in the CS (Leroy et al., 2006, 2011).

Using four short sediment cores (36–166 cm long) and 27 surface samples taken in the south basin and adjacent areas, the aims of this paper are (1) to establish a first spatial distribution pattern of dinoflagellate cysts in the Caspian area, especially the south basin and (2) to detect and explain changes over the last century in dinocyst assemblages and set it in the context of the Holocene – Neocaspian period. Prime focus will be on the autotrophic dinocyst *Lingulodinium machaerophorum* (Deflandre and Cookson, 1955) Wall, 1967, subsequently called *Lm* which is a euryhaline coastal planktonic species restricted to regions with summer temperatures above 10–12 °C (Marret et al., 2004) and winter temperatures above 0 °C (Marret and Zonneveld, 2003; Lewis and Hallett 1997). Its motile form, *Lingulodinium polyedra* (Stein) Dodge 1989, is reported to cause harmful algal blooms (Howard et al., 2009). This species therefore is sensitive to sea surface temperature and could be used to reflect climatic change in the region.

The impact of this work is important in advancing knowledge of Caspian Sea processes. The Caspian Sea holds a dominant position in the Southwestern Asian region, and is suspected of playing a major part in climate change in this part of the world. However, a lack of a clear understanding of the processes involved in its control such as the North Atlantic Oscillation or the El-Niño Southern Oscillation still exists not only for the last few millennia but also for the last few decades (Arpe et al., 2000, 2012; Arpe and Leroy, 2007). This paper addresses the issue of past temperatures and develops basic data that will underpin future work on Caspian Sea climate-related aspects.

BGD
9, 16663–16704, 2012

2 Setting

2.1 Geographical setting and climate

The CS is the world's largest inland water body in terms of both area and volume, extending 35–48° N and 47–55° E. The altitude of the surface lies around 26 m b.s.l. (25 to 29 m b.s.l. during the last 150 yr) (Arpe et al., 2012; Leroy et al., 2006). The sea is divided into three basins, becoming deeper southwards: the northern basin (80 000 km^2) with an average depth of 5 m and a maximum depth of 15 m; the middle basin (138 000 km^2) with an average depth of 175 m and a maximum depth of 788 m; and the Southern basin (168 000 km^2) with an average depth of 325 m and a maximum depth of 1025 m. The southern basin holds more than 65 % of the Caspian water.

Because of its great meridional extension (> 1100 km), the CS straddles several climatic zones (Kosarev, 2005). The northern part of the drainage basin lies in a zone of temperate continental climate with the Volga catchment well into the humid mid-latitudes. The western coast features a moderately warm climate, while the southwestern and the southern regions fall into a subtropical humid climatic zone. The eastern coast has a desert climate.

2.2 Currents, salinity and temperature

A complex sea current pattern in the middle and south basins is dominated by a surface cyclonic gyre (Zenkevitch, 1963). Specifically in the South Caspian a dipole system, consisting of an anticyclonic gyre in its northwestern part and a cyclonic gyre in its southeastern part, exists throughout the year (Zaker et al., 2011). The sea currents influence the four studied sites as they have potential to transport fine-grained materials. In contrast to the east coast of the middle basin, no upwelling develops in the south basin (Tuzhilkin and Kosarev, 2005).

In general, at the scale of the CS, the summer gradient of salinity is stronger than that of the winter. The main influences are, on an otherwise relatively stable salinity around

BGD
9, 16663–16704, 2012

11–12, the freshening influence of the Volga River in the north basin (salinities less than 1), and the stronger evaporation in the southeast (salinities up to 14) (Kosarev and Yablonskaya, 1994; Dumont, 1998). Monitoring from 1956 to 2000 shows high salinities in the early 1970s and low salinities in the early 1990s, corresponding respectively to low annual river discharge and high annual river discharge as well as the 1977 lowstand and the 1995 highstand (Fig. 2a). This water level change caused respectively a mixing of the water column and a stratification of the water column (Tuzhilkin and Kozarev, 2005). In the south basin, the summer and winter gradients show that the west is fresher (12.2) and the east more saline (13.8).

In the CS, summer temperature varies from 26 °C in the NW to > 28 °C in the SE. Winter temperatures are 10 °C in the centre of the basin and get cooler by 2 to 3 °C towards the periphery. A record of sea surface temperature in the south CS from 1982 to 2011 obtained by satellite) (Fig. 2b) shows a clear warming trend for all seasons (0.10 °C yr^{-1}) by 1–2 °C and stronger for the south basin of the Caspian than the other regions (Ginzburg et al., 2005 updated by European Centre for Medium-Range Weather Forecasts, ECMWF). The warming is the strongest for the summer with an increase from a little less than 25 °C to more than 28 °C. The extreme summer maxima show the strongest increase (Ginzburg et al., 2005). Moreover, based on hydrological data, a positive trend in the period 1900–1982 has been found but not as fast as after 1982 (Ginzburg et al., 2005). Thus the warming trend is independent of the significant sea level fluctuations that have taken place during the 20th century. A similar effect was observed in the Black Sea, Aral Sea and the Karabogaz-Gol by Ginzburg et al. (2005). These authors suggest that this warming trend could be a consequence of global warming (Fig. 2c). The sea ice season and extent in the northern basin have decreased for the period 1978 to 2002, also possibly related to global warming (Kouraev et al., 2004). For two out of the four coring locations more local information is provided in Appendix A.

BGD
9, 16663–16704, 2012

2.3 Nutrients and phytoplankton

Most *nutrients* enter the CS in the northern basin via the Volga River. The relatively low nutrient levels in the upper 100 m are depleted by phytoplankton activity, but the nutrient concentrations increase with depth (Kosarev and Yablonskaya, 1994). Iranian lagoons and coastal regions have however been steadily polluted by anthropogenic sources (fertilizers and pesticides used in agriculture and increased nutrient load of river flows due to deforestation of woodland) since the early 1980s (Kideys et al., 2008). For two out of the four coring locations more local information is provided in Appendix A.

Changes in phytoplankton biomass are one way to assess changes in water quality. Kideys et al. (2008) detected by satellite imagery an increase in chrolorophyll *a* in the southern CS since 2001. The invasion of the comb jelly *Mnemiopsis leidyi* in the late 1990s caused a drop in zooplankton, which in turn favoured phytoplankton. But other factors such as overfishing, eutrophication and climatic change may also have played a role.

Because of the pollution and because of the introduction of *M. leidyi*, the status of the south coast of the CS has changed between 1994 and 2005 from oligotrophic to meso-eutrophic, and the balance between diatoms, cyanobacteria and dinoflagellates shifted in favour of the latter two (Nasrollahzadeh et al., 2008a,b).

In 2006, an anomalous algal *bloom* mostly due to a dinoflagellate *Heterocapsa,* occurred in front of Anzali harbour (Bagheri et al., 2011). Other algal blooms mostly due to the toxic Cyanobacteria *Nodularia spumigna* occurred in August and September 2005 (20 000 km^2 of the southern basin) (Soloviev, 2005) in August 2009 (off Tonekabon) and in July and early August 2010 (from Nowshahr to near Babolsar and offshore Anzali) (Nasrollahzadeh et al., 2011; Makhlough et al., 2011). It is noteworthy that *L. polyedra* contributed significantly to the 2009 bloom (Nasrollahzadeh et al., 2011).

BGD
9, 16663–16704, 2012

2.4 Sediment sources and sedimentation rates

At present, rivers flowing to the Northern Caspian Coast (the Volga, Ural, Terek and Sulak) supply approximately 90 % of the riverine water influx to the CS, whereas the southwestern and southern rivers (the Sefidrud, Kura and Gorganrud) are the main sources of sediments for the whole of the CS (Lahijani et al., 2008).

Studies of the CS sediment composition have so far focused on the northern basin, where the proportions of the different inputs were estimated to be 35 % fluvial, 28 % aeolian, 29 % biogenic carbonate and 8 % chemical carbonates (Khrustalyov and Artiukhin, 1992). The Iranian mountains, such as the Elburz Mountain, represent the main source of terrigenous materials in the south basin. The sediment has two main primary detrital sources, more siliclastic in the west, more carbonates in the east (Lahijani and Tavakoli, 2011). One other source is aeolian transport by numerous dust storms from Turkmenistan, where Mesozoic limestones exist in the Kopet Dag (Lahijani and Tavakoli, 2011).

The south part of the basin was subsiding at a rate of the order of $> 1\,\mathrm{mm\,yr^{-1}}$ (Einsele and Hinderer, 1997) and this is probably still the case today.

The sedimentation rates in the south basin have always been very high due to its large accommodation space, strong erosion of the surroundings and orogenesis as well as aeolian inputs. For the Cainozoic, the sedimentary deposits in the Southern Caspian basin are as much as 20–30 km thick, making it one of the deepest basins in the world. For the Pliocene-Quaternary time alone, 10 km of sediment have been deposited, providing an average accumulation rate close to $2\,\mathrm{mm\,yr^{-1}}$ (Nadirov et al., 1997; Tagiyev et al., 1997). The sedimentation rate of the Pliocene in the south basin (the Pliocene Productive Series) is even higher up to $4\,\mathrm{mm\,yr^{-1}}$ (Kroonenberg et al., 2005).

BGD
9, 16663–16704, 2012

2.5 Past dinocyst investigations in the Caspian Sea

Some modern samples from the Caspian region were published in Marret et al. (2004), which is also the reference paper for the description of new Caspian genus, species and forms. Five surface samples were studied for their dinocyst content in the lagoon of Anzali (Kazancıet al., 2004) (Fig. 1).

The dinocyst history of the area is poorly known from previous dinocyst investigations, although four records cover the last 300 yr at least (locations in Fig. 1): in the Amirkola and Anzali Lagoons (Leroy et al., 2011), in the Gomishan lagoon, S-E corner of the CS (Kakroodi et al., 2012) and in the Karabogaz Gol (Leroy et al., 2006).

3 Materials and methods

3.1 Collection of surface samples, coring and dating

Modern samples were derived from a combination of core tops, grabs and hand scooping (Table A1). Sixteen samples came from marine settings, two from lakes, and nine from lagoons (locations in Fig. 1) Two Usnel boxes (50 cm thick) were taken in the south basin, during a French–Russian oceanographic cruise (August 1994), on board a Russian military ship, rented for the sea cruise (Table A2). Box locations were in water depths of 13 m for core US01 and of 315 m for core US02. Cores from Usnel boxes were subsampled in PVC tubes on board and therefore contain the water–sediment interface. Two Kajak heavy gravity cores with a diameter of 5 cm, cores CS03 and CS10, were taken in 2007 from a boat rented by the Iranian National Institute for Oceanography (INIO) (Table A2).

Two of the four cores were dated by radionuclides, i.e. US02 and CS03. ^{210}Pb, ^{226}Ra and ^{137}Cs records were obtained. Samples of core US02 were analysed every cm for both ^{210}Pb and ^{137}Cs in the top 10 cm, then every 2 cm down to 16 cm (results in Leroy et al., 2007). A sample at 22 cm reaches background values. For core CS03, samples

BGD
9, 16663–16704, 2012

were taken at ca. 3 cm interval down to 60 cm and then at every ca. 8 cm interval. Dry samples were measured with a very low-background, high-efficiency well-type detector located in the underground laboratory of Modane in the French Alps (Reyss et al., 1995) where 1700 m of rock overburden reduces the cosmic radiation by 6 orders of magnitude.

3.2 Sedimentology

For the sedimentary analysis of the two Usnels cores, dried samples were homogenized and representative subsamples were taken for grain size analysis by a LS 13 320 Multi-Wavelength Particle Size Analyzer, ASTM standard calibrated. Organic matter and calcium carbonate contents were determined by loss-on-ignition, bulk samples were dried at 105 °C for 24 h, then heated to 550 °C for 4 h to burn the organic matter, and organiccarbon free sample heated again to 950 °C for 8 h to break the calcium carbonate. The percentages of organic matter and calcium carbonate were then calculated by the method used by Dean (1974).

For the two Kayak cores, samples were homogenized and representative subsamples were taken for grain size analysis. The distribution for the fraction coarser than 1 mm was determined using the standard wet sieving procedure. Grain-size analysis for particles less than 1 mm was undertaken using a "Fritsch Analysette Comfort 22" Laser Particle Sizer. Organic matter was determined by wet digestion through oxidation in hydrogen peroxide on bulk samples (Schumacher, 2002). The calcium carbonate was determined by using a Bernard calcimetre.

The magnetic susceptibility was measured with a Bartington Instruments MS2 susceptibility bridge. Cores CS03 and CS10 were measured using a MS2C sensor on half cores, core US01 using MS2E1 and core US02, using MS2F sensor, both along flat surface of half cores. The thermomagnetic behaviour of the bulk sediment sample from core US02, was determined on a horizontal force translation balance in air atmosphere in a magnetic field of 0.375 T and with a linear temperature increase.

BGD
9, 16663–16704, 2012

3.3 Palynology

Samples were taken every 5 cm in the four cores. Initial processing of samples (1 to 2 ml) involved the addition of sodium pyrophosphate to deflocculate the sediment. Samples were then treated with cold hydrochloric acid (10 % and then pure) and cold hydrofluoric acid (60 %), followed by a further treatment with hydrochloric acid. The residual organic fraction was then screened through 125 µm and 10 µm mesh sieves and mounted on slides in glycerol. *Lycopodium* tablets were added at the beginning of the process for concentration estimates.

The dinocysts were counted at the same time as pollen and other microfossils. The sum for percentages is made of all dinocysts except *Brigantedinium* spp. (including all "round-brown" specimens which are cysts not identified to the species level), because of its ubiquitous character and frequent dominance of the spectra. *Brigantedinium* and varia are expressed as a percentage of the same sum as the other dinocysts. The percentages of the foraminifera inner organic linings found in the palynological slides were displayed in the same way. A ratio pollen concentration on dinocyst concentration (P : D) has been determined according to McCarthy and Mudie (1998) in order to estimate the degree of continentality of the assemblage.

A statistical analysis available in Psimpoll (Bennett, 2007), the zonation by cluster analysis (CONISS) after square root transformation of the percentages, was applied. The zonation was calculated for the percentage diagrams.

The taxonomy of many Caspian dinocyst species has been established by Marret et al. (2004). Illustrations of Caspian dinocysts are also available in Leroy (2010) and Mudie et al. (2011). Three forms of *Lm* have been counted separately: ss, A and B. In a worldwide study, Mertens et al. (2009) indicate that *Lm* can be found in surface sediment in a salinity range from at least 12.5 to 42, and for temperature from 9 to 31 °C. The same study established that longer processes are clearly developed at higher summer salinity (Mertens et al., 2009) For the CS, the length of the processes decreases from form ss to form B.

BGD
9, 16663–16704, 2012

4 Results

4.1 The surface samples

The samples are organised by increasing percentage values of *Lm* B from the top to the bottom of Fig. 5, except the bottom two samples which have high values of forms ss and A.

At the top of the diagram, the assemblages of the two lake samples (Almagol and Alagol) are composed only of *Brigantedinium*. At the bottom of the diagram, the dinocysts are dominated by *Lm* B with increasing values of *Lm* ss and often the presence of *S. belerius* (saline lagoons of BTork 1 and 2, and TR1). The bottom-most two samples are derived from hypersaline settings: the Aral Sea (AS17-5) and the Karabogaz Gol (KBG8-01) explaining respectively the abundance of *Lm* ss and the high peak of *Lm* A.

In the middle sample group, the spectra are dominated by *I. caspienense* and *Caspidinium rugosum rugosum*, with occasionally at the top end of the diagram the development of *Pentapharsodinium dalei* and *S. cruciformis*, respectively in north of the middle Caspian basin (cores US24 and US26) or more freshwater lagoons (Anzali).

4.2 Core sediment and dating

The sediment of core US01, off the coast of Turkmenistan, is silty with up to 20 % clays. It has the highest amount of sand of the four cores, reaching 10–20 % (Fig. 4). The core bottom has 4 % organic matter, but this rapidly decreases upwards to 1 %. The carbonate content is stable around 20 %. The magnetic susceptibility is very low and increases upwards. Foraminifera tests are abundant (Appendix B).

The sediment of core *US02*, from the middle of the south basin, is clayey and silty with some sand from 8.5 % at the base to 2 % at the top. The organic matter progressively increases from 2 to 4 %. This sequence has the highest content in carbonates of the four cores, reaching 30–40 %. It is likely that some of the carbonate is derived

BGD
9, 16663–16704, 2012

from benthic ostracod valves as they are known in the top cm of this core (Boomer et al., 2005). The magnetic susceptibility is low. The Curie temperature for sample at 6 cm depth was 580 °C; the mineral carrying the magnetic susceptibility is magnetite (Fe_3O_4).

The sediment of core *CS03*, offshore from Anzali, is comprised of gray silts and clays with darker layers. The sediment is occasionally bioturbated by a network of animal tubes. The mean amounts of organic matter and carbonates are stable with respectively values of 3 and 17 %. The magnetic susceptibility is low.

The sediment of core *CS10*, taken offshore from Babolsar, consists of clayey silts, sometimes with very fine sand, poorly sorted, getting darker with depth, ranging from dark grey to black with a reduced-sediment odour. Sediments are laminated through much of the sequence. Some part of the sequence appears burrowed (particularly the lower portion). The sequence has 3 % of organic matter and 20 % of carbonates as well as the highest magnetic susceptibility of the four cores.

The radionuclide results of core US02 have been published in Leroy et al. (2007). In brief the sedimentation rate obtained is 2.0 mm yr^{-1} for the top 22 cm of sediment. The base of the core is therefore estimated to be at AD 1709.

For core CS03, the record of artificial fallout radionuclides ^{241}Am and ^{137}Cs (Fig. 5) detected in the upper 104 cm. of sediment display a maximum at 83 cm depth that is assigned to the period of maximum weapons fallout (Appleby, 2000) The corresponding averaged sedimentation rate is thus of 19 mm yr^{-1}. The radiometric ^{210}Pbexc profile (Fig. 5) does not display the regular exponential decrease with depth in the core as expected for a constant sedimentation rate. For the upper 63 cm, the profile exhibits a roughly linear decreasing activity corresponding to a sedimentation rate of 20 mm yr^{-1} in good agreement with the artificial radionuclide results. Deeper in the core, the data are more scattered and would correspond to a higher sedimentation rate. Assuming that the sedimentation rate of the deeper part of the core is higher than 20 mm yr^{-1}, the age of the base of the core is estimated between AD1963 and AD1930. The use of other models (CIC, CRS, Appleby 2000, and SIT, Carroll and Lerche 2003) was not

BGD
9, 16663–16704, 2012

attempted because of the large discontinuities in the sampling depths. The sedimentation rate that was obtained, 20 mm yr^{-1} is therefore exceptionally high and 10 times higher than that of core US02.

No dating is available for cores US01 and CS10. It is however likely that the sedimentation in front of the Babolsar River, for core CS10, will be similar or slightly lower than that of core CS03 because the Babolsar river (in front of the CS10 coring location) sediment discharge is minute when compared to that of the Sefidrud (a powerful river, but east of core CS03): 0.411 Mton yr^{-1} versus 26 000 Mton yr^{-1} (Lahijani et al., 2008).

4.3 Dinocysts in the four cores

In general the same range of taxa is found in the four cores (Fig. 6), with the usual dominance of *I. caspienense* and the abundance of *Lm* under two forms: B and ss (Marret et al., 2004). *P. psilata* has only rare occurrences.

4.3.1 Core US1, the shallow core off Turkmenistan

This sequence is largely dominated by only two taxa: *I. caspienense* whose percentages decrease slightly from 60 to 40 %, and *Lm* B whose percentages increase. *Lm* ss and *S. belerius* have continuous curves. The P : D ratio is very low (if compared to modern samples, Fig. 3) indicating that more dinocysts than pollen are preserved in the sediment and therefore that the continental influence is low despite the proximity of the continent and that the dinocysts have found optimal conditions to grow. Foraminifera linings have been found in significant numbers throughout the core and form a continuous curve.

4.3.2 Core US2, the last 300 yr in the middle of the south basin

Zone US02-d1 has relatively high *S. cruciformis* values and a significant percentage of *C. rugosum,* not met in the surface samples. Zone US02-d2 has slightly less *S. cruciformis*, much less *C. rugosum* and slightly more *Lm* B.

BGD
9, 16663–16704, 2012

The concentration is the lowest of the four cores due to the distance to the shores. The relatively low P : D displays an increasing overall trend. This diagram shows a mild trend to have opposite fluctuations of *P. dalei* cysts (highest values of the 4 cores) and *Lm* B. This core overall shows assemblages that indicate the lowest salinities of the four cores. This is due to its location in a more open sea. No foraminifera linings have been found in this sequence as the water depth is too great for the survival of these benthic organisms in the CS (Boomer et al., 2005).

4.3.3 Core CS03, the 20th century off Anzali

In zone CS03-d1 *I. caspienense* has maximal values, *P. dalei* cysts are well represented and the percentages of *Brigantedinium* are relatively high. The concentration increases slowly and the P : D decreases upwards. In zone CS03-d2, *Lm* B values are nearly twice as high as before. *P. dalei* cysts become rare. The concentration is clearly higher than in zone 1, while P : D is stable. This core shows a compelling opposition between *P. dalei* cysts and *Lm* B.

The coring location 15 km offshore, does not seem to be influenced by the freshwater outflow from the Anzali lagoon.

4.3.4 Core CS10, with massive algal biomass increase off Babolsar

In zone CS10-d1, the values of *I. caspienense* are the highest of the four cores. The P : D is extremely high: showing a clear terrestrial influence similar to that in surface samples, e.g. in lakes (such as Alagol) and lagoons (Anzali and Bandar-e-Torkman).

In zone CS10-d2, after a sudden change, high percentages of *Lm* B (80 %) occur. These are also the highest values ever recorded in the CS. This occurs in parallel to a huge increase in the dinoflagellate cyst biomass.

The limit between zones CS03-d1 and d2 corresponds well to that between zones CS10-d1 and d2, with the same increase in *Lm* B and ss percentages and in total biomass and the same decrease in *Brigantedinium* and in the P/D ratio. This change at

BGD
9, 16663–16704, 2012

75 cm is well dated in core CS03 as it is just a few cm above the ^{237}Cs peak of AD1963 at 83 cm, bringing the age of the limit at AD1967.

5 Discussion

5.1 Dinocyst distributions

The spectra from the surface sediment and the four cores are largely dominated by *I. caspienense* and *Lm*. The near absence of *P. psilata* and the low values of *S. cruciformis* (for the latter except the central core and some surface samples in the Lagoon of Anzali) are a characteristic of these four recent records and of the surface samples. *P. psilata* is mostly found in Khvalynian sediment (Leroy, personal communication, 2012) and in lagoons and river deltas such as the Demchik area of the Lower Volga River (K. Richards, personal communication, 2012). This is easily explained both in terms of the higher salinity of the Neocaspian Sea and in terms of survival in lagoons where the salinity is variable and where the lagoons maintain at most times at least small areas of lower salinity if fed by rivers. The higher values of *S. cruciformis* in zone US02-d1 may reflect the much higher water levels of the LIA, which also have less saline waters as also seen in the lagoon of Anzali (Leroy et al., 2011).

The two southern cores have the highest percentages of *Brigantedinium*. This is explained by the proximity of a densely inhabited coastal area producing a lot of nutrients discharged into the sea.

The cosmopolitan species *P. dalei* cyst is clearly more abundant in the northern surface samples (samples US24 and 26), which are characterised by larger amplitudes of sea surface temperatures and the proximity of sea ice in winter (Marret et al., 2004).

On the one hand, based on the locations of the cores and the surface samples, it is possible to show that the three *Lm* forms show an increasing salinity gradient from B, to ss and finally to A. On the other hand, *Lm* percentages (all forms included) display an increase across the CS to the southeast, i.e. towards regions that are warmer and

BGD
9, 16663–16704, 2012

more saline. So the morphology of the cysts responds to the salinity but its biomass to temperature.

5.2 Exceptional sedimentation rate

The sedimentation rate of core US02, in the centre of the south basin, obtained by the radionuclide method is 2 mm yr^{-1}. This is 10 times higher than that obtained by radiocarbon on core CP14 taken close by (Leroy et al., 2007). This difference could be caused not only by an expected lack of compaction of the top tens of cm of sediment in core US02 but also by a very recent (the last few centuries) increase of the sedimentation influx (Leroy et al., 2007). This radiocarbon-based value falls within the sedimentation rates of other cores from the deep basins i.e. between 0.02 and 0.54 mm yr^{-1} (Amini et al., 2012).

The sedimentation rate in a short core (HCGA05, 170 cm long) from the Anzali Lagoon, is of 5 mm yr^{-1}, that of core HCGL02 (95 cm long) in the lagoon of Amirkola is 2.5 mm yr^{-1} (Leroy et al., 2011), and that in cores from the Gorgan Bay is between 1.4 and 2.45 mm yr^{-1} (Karbassi and Amirnezhad, 2004). These values are higher than those from the core from the centre of the south basin. These lagoonal settings are expected to have higher sedimentation rates than those of the open sea.

On the whole the values of the short cores are in the order of the sedimentation for the Cainozoic (Nadirov et al., 1997; Tagiyev et al., 1997).

However 20 mm yr^{-1} obtained on the coastal core CS03 is truly exceptional (Amini et al., 2012). This value is even higher than that of the Pliocene Productive Series (Kroonenberg et al., 2005). This is explained by the core location on the slope of the continental shelf. The time resolution of the palynological samples therefore reaches one sample every 2.5 yr.

BGD
9, 16663–16704, 2012

5.3 Shifts in the *L. machaerophorum* percentages

This section focuses on what causes the increase in *Lm* visible in the four cores, more so for the two southern ones (Figs. 6, 7). Moreover these increases of *Lm* are often to the detriment of *P. dalei* cysts when present in the cores. The recent changes are then set in the context of the changes in the last few millennia.

5.3.1 In the last decades

L. polyedra, the motile form of *Lm* usually occurs in the water column during late summer, which suggests that a minimum temperature is needed for its development. *L. polyedra* can bloom in nutrient rich and nutrient depleted waters: thus its distribution does not have to be restricted to areas with high nutrient concentrations in surface waters (Lewis and Hallett, 1997). Dinoflagellate biomass that shows a steep increase as part of anomalous algal blooms that occurred in the last few years in the CS are probably seen in the strong algal biomass increase across core CS10, especially since 1967. The causes for this are multiple, and are often attributed to nutrient washed into the sea by the rivers; however they are also often linked to higher temperature and low wind conditions and therefore stratified waters (Soloviev, 2005; Nasrollahzadeh et al., 2011). A remote sensing analysis for the 2005 large-scale bloom indicated that an increase of 4 °C was observed in the bloom itself in comparison to surrounding waters. Low wind conditions and water stratification were also observed. In brief this would tend to indicate that *L. polyedra* responds primarily to high temperatures, with salinity, and nutrients as secondary factors.

In the 20th century, the water level has fluctuated by ±3 m a couple of times (Fig. 2a), but this seems to have been hardly registered in the fossil record (Fig. 6). More decisively, the sharp sea level rise between 1977 and 1995 has led to a salinity decrease. However *Lm* percentages have strongly increased, more in line with the gradual increase of sea surface and air temperatures throughout this period (Fig. 2b–d)

BGD
9, 16663–16704, 2012

5.3.2 In the Late Holocene

Successive dinocyst phases are characterised by the dominance of various dinocysts in the later part of the Late Pleistocene–Holocene history of the CS: (1) the most recent is a *Lm* phase in the last few decades, (2) the next one is dominated by *I. caspienense* until ca. 3.9 cal. ka ago, and (3) the oldest one, covering the early Holocene and Late Pleistocene, is dominated by *S. cruciformis* and *P. psilata*. This succession was already suspected in core CP14 (Leroy et al., 2007), but it is only with the additional cores US01, US02, CS03 and CS10 that the most recent phase became clearly visible.

The examination of thirteen records reveals the following history in the development of *Lm* (Figs. 1, 7). It is quasi absent from a 10 m long core in the centre of the south basin, core GS05, whose top reaches ca. 4000 yr ago (Pierret et al., 2012; Leroy, personal communication, 2012) and only present in the top cm of a 10 m long core in the centre of the middle basin, core GS18, from ca. 2900 yr ago onwards (Boomer et al., 2005; Leroy, personal communication, 2012). In the Holocene lagoonal core TM in Gomishan, SE of the south basin, *Lm* starts to develop only from ca. 3200 yr ago (Kakroodi et al., 2012). In the marine cores CP14, 18 and 21 covering most of the second half of the Holocene (Leroy et al., 2007), a steady increase is observed. More especially in core CP14, *Lm* starts to develop ca. 2500 yr ago (Leroy et al., 2007). The other much shorter records, KBG08, HCGL02 and HCGA05, show the abundance of this dinocyst in the last few centuries (Leroy et al., 2006, 2011). In core HCGA05, Anzali Lagoon (Leroy et al., 2011), *Lm* fluctuates in anti-phase with *S. cruciformis*; this was interpreted as a salinity signal. The highest percentages of *Lm* B, 80 %, and *Lm* A, 80 %, are respectively found in core CS03 (Iranian coast) and in the Karabogaz-Gol.

Contrary to the CS, in the Black Sea, *Lm* is already present at the beginning of the Holocene. In the SW of the Black Sea, *Lm* occurs in cores M02-45 and MAR05-13 respectively over the last 9500 uncal. ^{14}C years and 11 000 uncal. ^{14}C years (Marret et al., 2009; Bradley et al. 2012) (note that the Black Sea radiocarbon dates are often uncalibrated and uncorrected for the reservoir effect due to major uncertainties). From

BGD
9, 16663–16704, 2012

6 uncal. ^{14}C ka, it is even largely dominant. It peaks from 6 to 5 uncal. ^{14}C ka, which is considered the warmest period in the climate of the Black Sea region. The topmost part of the core estimated to be close to the present shows at least 80 % of *Lm* ss. Marret et al. (2009) suggested that these high values were due to anomalous blooms of this species.

In a Marmara Sea sedimentary sequence, Verleye et al. (2009) found an opposition similar to that of the present study between *Lm* and *P. dalei* cysts interpreted here as less river input versus higher terrigenous input. In the Sea of Barents, the abundance of cysts of *P. dalei* increases according to Voronina et al. (2001) near high productivity waters. An investigation of dinocysts in a core from the Marmara Sea covering the Late Pleistocene and Holocene considers *Lm* as a thermophilous taxon (Londeix et al., 2009).

In brief in the CS, contrary to the Black Sea, it appears that the *Lm* development started slowly only ca. 3200 yr ago and has strongly accelerated in the last decades.

The causes of this appearance and development of *Lm*, are not sea levels that have fluctuated widely during that time period. During the LIA, the water level was 6 m higher than at present (archaeological and documentary evidences in Brückner, 1890; palaeoenvironments in Leroy et al., 2011). During the early Middle Ages, the water levels were lower by 2–4 m as attested by the numerous walls built by the Sasanian Empire (archaeological and documentary evidences in Brückner, 1890; Omrani et al., 2007). A high stand similar to the LIA has been recorded between 2600 and 2300 cal. yr BP (sediment in Kroonenberg et al., 2007; Kakroodi et al., 2012). These important changes have so far not been recorded in the *Lm* curve.

Causes for the increase in *Lm* percentages and biomass should be sought more in a regional signal such as a possible long-term recovery from glacial meltwater inflow (Leroy et al., 2007) or at a global level.

BGD
9, 16663–16704, 2012

5.4 *L. machaerophorum* increase and sea surface trends

Changes in phytoplankton abundance may be driven by several factors that may confound the climatic signal (Adrian et al., 2009). In the present situation, it is however possible to eliminate two important factors that may have explained the changes in *Lm*: sea level changes, hence salinity, and also eutrophication. Indeed (1) sea level changes have taken place in the last millennia and even centuries but did not affect the percentages of *Lm*; and (2) because the shift to increased values of *Lm* is older than anthropogenic eutrophication and because here *Lm* is inversely correlated to *P. dalei*, eutrophication may be secondary only in explaining the CS trend.

The temperature trend across the later part of the Holocene, due to a long-term recovery from the end of the meltwater inflow into the CS, is the initial forcing factor. The recent global warming trend detected in the CS 20th century instrumental data (air and sea surface), and confirmed for the first decade of the 21st century (Fig. 2b–d), has fuelled the further increase of *Lm*.

In brief, it has been shown that the increase of *Lm* is due first to natural global and/or regional climatic forcing working at the millennial timescale, such as a long-term recovery from meltwater inflow, and secondly it was amplified by a recent warming of the surface waters likely related to a recent anthropogenic-induced global forcing in the last decades. The temperature increase is the primary forcing factor, and salinity increase is just a corollary, reinforced by the closed basin setting.

6 Conclusions

This study is the first to provide an analysis of modern and very recent dinocyst assemblages for the Caspian Sea, with more details for the south basin in some cores with exceptional sedimentation rates.

This investigation of surface samples has provided a baseline for the present state of the CS and surroundings, with the dinocysts reflecting water parameters. This may

BGD
9, 16663–16704, 2012

serve as a reference when comparing it with past states and future ones. More specifically for the present, the following was observed: more *P. dalei* cysts in the north at proximity to winter sea ice and with larger seasonal contrasts, more *S. cruciformis* in freshwater lagoons or in the oligohaline north, and more *Lm* in the warmer south and in higher salinity settings.

New analyses of four short cores in the CS have shown a recent expansion of the dinoflagellate cyst *Lm*. This species of dinoflagellate could be taken as an indicator of sea surface temperature. When these results are placed in the context of thirteen sequences in the CS, a robust signal is obtained: the dinocyst trend is the end result of a natural increase that has started two or three millennia ago in the Holocene. The overall trend has recently been amplified by global warming as shown by instrumental data. This warming has significantly changed the dinocyst assemblage in the CS.

The dinocyst assemblages and the sea surface temperatures indicate that the CS has moved into the Anthropocene (Crutzen, 2002) as many other lakes (Adrian et al., 2009). The CS is a fragile ecosystem exploited by multiple users who each wish to sustain their economical development and who will have to change in order to adapt to the present changes.

Appendix A

Modern oceanographic parameters for Anzali and Babolsar

Offshore from Anzali (one of the four main studied locations, S-SW Caspian coast of Iran, Fig. 1) across the four seasons of the year 2006, the temperature and salinity profiles at a station with 50 m water depth indicate a constant temperature down to 30 m followed by a thermocline (26 to 9 °C). The salinity (9.32 and 12.25) is also constant, with just a drop in surface waters in February (Bagheri et al., 2011).

The temperature structure offshore from Babolsar (close to another one of the four main studied locations, S-SE Caspian coast of Iran, Fig. 1) is characterized by a strong

BGD
9, 16663–16704, 2012

seasonal thermocline, located between 20 and 50 m depth with a 15 °C temperature difference across it in summer. In autumn, the thermocline gradually weakens and, at the end of winter, it disappears before its re-formation in the early spring. The salinity is 12 with a slight decrease to 11 in enhanced river flow to the sea (Zaker et al., 2007, 2011).

Temperature and salinity measurements along the Iranian coast show similar temperatures but with slightly wider seasonal amplitude in the west (Table A1). The salinity increases eastwards because of the inflow of freshwater in the west via Anzali lagoon and the Sefidrud River.

No sewage control exists in Babolsar: industrial, domestic and agricultural wastes go to the sea via the river. Moreover, in both the flat coastal plains of Anzali-Rasht and Babolsar, a significant source of nutrients is derived from the fertilizers used in the rice fields

Appendix B

The analysis of foraminifera tests in core US01

B1 Materials and methods

Due to the continuous presence of foraminifera linings in palynological slides, core US01 was selected for foraminifera test analyses. Seven samples were taken at approximately 5 cm intervals. The samples were dried at 50 °C in an oven and weighed. Subsequently the samples were treated with a 4 % solution of H_2O_2 for 15 h and were wet sieved through mesh sizes of 53, 63, 125, 250 µm and then were dried again. Afterwards, all foraminifera were picked and identified from 53, 63, 125 and 250 µm fractions under a binocular microscope and finally percentages were calculated for each species. In the case of samples rich in foraminifera, the samples were split into 1/8 prior to sieving, then picked and the total abundances were then calculated by multiplying.

BGD
9, 16663–16704, 2012

The taxonomic classification followed the suprageneric taxonomy of Loeblich and Tappan (1987), with some information from Birshtein et al. (1968).

B2 Results

The sediment contains five different euryhaline benthic foraminifera taxa: *Ammonia beccarii* (47–87 %), *Elphidium littorale* (also known as *Elphidium littorale caspicum, Retroelphidium littorale, Retroelphidium caspicum, Elphidium caspicum caspicum* and *E. gunteri*) (10–52 %), *Elphidium shochinae* (0.9–0.83 %), *Elphidiella brotzkajae* (0.6–4.87 %) and *Cornuspira sp.*(0.11 %) (Fig. D1). *Ammonia beccarii* is the most abundant taxon in this core and *Elphidium shochinae* and *Cornuspira sp.* are the rarest.

The comparison of foraminifera abundance between the four fractions shows a maximum abundance in the 63–125 and 125–250 µm fractions. The maximal abundance of foraminifera is at 24 cm depth, with assemblages displaying a dominance by *Ammonia beccarii.* The lowest foraminifera concentration is recorded at 7 cm depth (Fig. D1). In the entire core, *A. beccarii* maximum abundance is at 14 cm depth and minimum abundance at the 34 cm of core, but the abundance of *E. littorale* is reversed at these depths.

The core US01 is characterized by silty sediments with sand and clay with low organic matter except below 27 cm depth where it reaches 5 %. *A. beccarii* dominates this core and is indicative of a shallow-marine environment with sandy bottom (Sgarrella and Moncharmont Zei, 1993). However below 20 cm depth, *Elphidium littorale* is more abundant and this could be paralleled to the higher organic matter values.

BGD
9, 16663–16704, 2012

Acknowledgements. Our gratitude goes to F. Gasse, the leader of the project "Understanding the Caspian Sea erratic fluctuations", European Contract INCO-Copernicus no. IC15-CT96-0112, to F. Guichard and P. Tucholka for collection of Usnel box cores, to P. J. Giannesini and E. Moreno, past and present curators of cores from the Caspian Sea (Laboratoire de Géologie, Museum d'Histoire Naturelle de Paris, France). We are grateful to M. Naderi (INIO) who helped in the field. The Golestan samples were kindly provided by A. A. Kakroodi. All the palynological samples were treated at Brunel University by C. Miller, who also made the magnetic susceptibility measurements of the two Kajak cores. This article is a contribution to the European project Marie Curie, CLIMSEAS-PIRSES-GA-2009-247512: "Climate Change and Inland Seas: Phenomena, Feedback and Uncertainties. The Physical Science Basis". S. Kershaw and L. López-Merino (Brunel University) have provided critical feedback on earlier versions of the manuscript.

References

Adrian, R., O'Reilly, C. M., Zagarese, H., Baines, S. B., Hessen, D. O., Keller, W., Livingstone, D. M., Sommaruga, R., Straile, D., Van Donk, E., Weyhenmeyer G. A., and Winder, M.: Lakes as sentinels of climate change, Limnol. Oceanogr., 54, 2283–2297, 2009.

Amini A., Mousavi Harami, R., Lahijani, H., and Mahboubi, A.: Holocene sedimentation rate in Gorgan Bay and adjacent coasts in southeast of Caspian Sea, J. Basic Appl. Sci. Res., 2, 289–297, 2012.

Appleby, P. G.: Radiometric dating of sediment records in European mountain lakes, J. Limnol., 59, 1–14, 2000.

Arpe, K. and Leroy, SAG: The Caspian Sea Level forced by the atmospheric circulation as observed and modeled, Quatern. Int., 173–174, 144–152, 2007.

Arpe, K., Bengtsson, L., Golitsyn, G. S., Mokhov, I. I., Semenov, V. A., and Sporyshev, P. V.: Connection between Caspian Sea level variability and ENSO, Geophys. Res. Lett., 27, 2693–2696, 2000.

Arpe, K., Leroy, S. A. G., Lahijani, H., and Khan, V.: Impact of the European Russia drought in 2010 on the Caspian Sea level, Hydrol. Earth Syst. Sci., 16, 19–27, doi:10.5194/hess-16-19-2012, 2012.

BGD

9, 16663–16704, 2012

Bagheri, S., Mansor, M., Makaremi, M., Sabkara, J., Wan Maznah, W. O., Mirzajani, A., Khodaparast, S. H., Negarestan, H., Ghandi, A., and Khalilpour, A.: Fluctuations of phytoplankton community in the coastal waters of Caspian Sea in 2006, Am. J. Appl. Sci., 8, 1328–1336, 2011.

Bennett, K.: Psimpoll and pscomb programs for plotting and analysis, Version psimpoll 4.27, available at: http://chrono.qub.ac.uk/psimpoll/psimpoll.html (last access: 26 July 2012), 2007.

Birshtein, Y. A., Vinogradov, L. G., Kondakov, N. N., Astakhova, M. S., and Romanova, N. N. (Eds.): Atlas of Invertebrates of the Caspian Sea, Pishchevaya Promyshlennost, Moscow, 1968 (in Russian).

Boomer, I., Hoorne, D., and Slipper, I. J.: The use of ostracods in palaeoenvironmental studies, or what can you do with an ostracod shell?, Paleontol. Soc. Papers, 9, 153–179, 2003.

Boomer, I., von Grafenstein, U., Guichard, F., and Bieda, S.: Modern and Holocene sublittoral ostracod assemblages (*Crustacea*) from the Caspian Sea: a unique brackish, deep-water environment, Palaeogeogr. Palaeocl., 225, 173–186, 2005.

Bradley, L., Marret, F., Mudie, P., Aksu, A., and Hiscott, R.: Constraining Holocene sea-surface conditions in the southwestern Black Sea using dinoflagellate cysts, J. Quaternary Sci., 27, 835–843, doi:10.1002/jqs.2580, 2012.

Brückner, E.: Klima-Schwankungen seit 1700 nebst Bemerkungen über die Klimaschwankungen der Diluvialzeit. Geographische Abhandlungen herausgegeben von Prof. Dr Albrecht Penck, E. Hölzel, Vienna and Olmütz IV (2), 153–484, 1890.

Carroll, J. and Lerche, I.: Sedimentary Processes: Quantification Using Radionuclides, Elsevier, Oxford, 2003.

Cazenave, A., Bonnefond, K., Dominh, K., and Schaeffer, P.: Caspian Sea Level from Topex-Poseidon altimetry: level now falling, Geophys., Res., Lett., 24, 881–884, 1997.

Climatic Research Unit: University of East Anglia, avaiable at: http://www.cru.uea.ac.uk/cru/data/temperature/crutem4/station-data.htm, last access: 30 August 2012.

Crétaux, J.-F. and Birkett, C.: Lake studies from satellite radar altimetry, C. R. Lake studies from satellite radar altimetry C. R. Geosci., 338, 1098–1112, 2006.

Crutzen, P. J.: Geology of mankind, Nature 415, 23, doi:10.1038/415023a, 2002.

Dean Jr., W. E.: Determination of carbonate and organic matter in calcareous sediments and sedimentary rocks by loss on ignition: comparison with other methods, J. Sed. Petrol., 44, 242–248, 1974.

BGD

9, 16663–16704, 2012

Dee, D. P., Uppala, S. M., Simmons, A. J. et al.:The ERA-Interim reanalysis: configuration and performance of the data assimilation system, Q. J. Roy. Meteor. Soc., 137, 553–597, doi:10.1002/qj.828, 2011.
Deflandre, G. and Cookson, I. C.: Fossil microplankton from Australia late Mesozoic and Tertiary sediments, Aust. J. Mar. Fresh. Res., 6, 242–313, 1955.
Dumont, H. J.: The Caspian Lake: history, biota, structure, and function, Limnol. Oceanogr., 43, 44–52, 1998.
Einsele, G. and Hinderer, M.: Terrestrial yield and the lifetimes of reservoirs, lakes and larger basins, Geol. Rundsch., 86, 288–310, 1997.
Firoozfar, A., Bromhead, E. N., Dykes, A. P., and Neshaei, M. A. L.: Southern Caspian Sea coasts, morphology, sediment characteristics, and sea level change, in: Proceedings of the Annual International Conference on Soils, Sediments, Water and Energy, 17,123–150, 2012.
Ghaffari, P., Lahijani, H. A., and Azizpour, J.: Snapshot observation of the physical structure and stratification in deep-water of the South Caspian Sea (western part), Ocean Sci., 6, 877–885, doi:10.5194/os-6-877-2010, 2010.
Ginzburg, A. I., Kostianoy, A. G., and Sheremet, N. A.: Sea surface temperature variability, in: The Caspian Sea Environment, edited by: Kostianoy, A. and Kosarev, A., Springer, Berlin, Heidelberg, 59–81, 2005.
Golitsyn, G. S. and Panin, G. N.: The water balance and modern variations of the level of the Caspian Sea, Soviet Meteorol. Hydrol. (English Translation) 1, 46–52, 1989.
Howard, M. D. A., Smith, G. J., and Kudela, R. M.: Phylogenetic relationships of Yessotoxin-producing dinoflagellates, based on the large subunit and internal transcribed spacer ribosomal DNA domains, Appl. Environ. Microbiol., 75, 54–63, 2009.
Jamshidi, S. and BinAbuBakar, N.: Oceanographic study in coastal waters in Babolsar, Asian J. Earth Sci., 4, 1–8, 2011.
Kakroodi, A. A., Kroonenberg, S. B., Hoogendoorn, R. M., Mohammadkhani, H., Yamani, M., Ghasssemi, M. R., and Lahijani, H. A. K.: Rapid Holocene sea-level changes along the Iranian Caspian coast, Quatern. Int., 263, 93–103, 2012.
Kakroodi, A. A., Leroy, S. A. G., Kroonenberg, S. B., Lahijani, H. A. K., Alimohammadian, H., Yamani, M., and Nohegar, A.: Late Pleistocene and Holocene sea level-change and coastal palaeoenvironment along the Iranian Caspian shore, Earth Planet. Sci. Lett., submitted, 2012.

BGD
9, 16663–16704, 2012

Karbassi, A. R. and Amirnezhad R.: Geochemistry of heavy metals and sedimentation rate in a bay adjacent to the Caspian Sea, Int. J. Environ. Sci. Te., 1, 191–198, 2004.
Kazancı, N., Gulbabazadeh, T., Leroy, S. A. G., and Ileri, O.: Sedimentary and environmental characteristics of the Gilan-Mazenderan plain, Northern Iran: influence of long- and short-term Caspian water level fluctuations on geomorphology, J. Mar. Syst., 46, 145–168, 2004.
Khrustalyov, Y. P. and Artiukhin, Y. V.: Sedimentation in the southern inland seas of the arid zone of the USSR, Mar. Geol., 103, 503–512, 1992.
Kideys, A. E., Roohi, A., Eker-Develi, E., Mélin, F., and Beare, D.: Increased chlorophyll levels in the Southern Caspian Sea following an invasion of jellyfish, Res. Lett. Ecol., 2008, 185642, doi:10.1155/2008/185642, 2008.
Kosarev, A. N.: Physico-geographical conditions of the Caspian Sea, in: The Handbook of Environmental Chemistry, edited by: Hutzinger, O., vol. 5 water pollution, Pt. P, Springer, Berlin, 5–31, 2005.
Kosarev, A. N. and Yablonskaya, E. A.: The Caspian Sea, SPB Academic Publishing, The Hague, 259 pp., 1994.
Kouraev, A. V., Papa, F., Mognard, N. M., Buharizin, P. I., Cazenave, A., Cretaux, J.-F., Dozortseva, J., Remy, F.: Sea ice cover in the Caspian and Aral Seas from historical and satellite data, J. Mar. Syst., 47, 89–100, 2004.
Kroonenberg, S. B., Simmons, M. D., Alekseevski, N. I., Aliyeva, E., Allen, M. B., Aybulatov, D. N., Baba-Zadeh, A., Badyukova, E. N., Davies, C. E., Hinds, D. J., Hoogendoorn, R. M., Huseynov, D., Ibrahimov, B., Mamedov, P., Overeem, I., Rusakov, G. V., Suleymanova, S., Svitoch, A. A., and Vincent, S. J.: Two deltas, two basins, one river, one sea: the modern Volga delta as an analogue of the neogene productive series, South Caspian Basin, river deltas – concepts, models, and examples (SEPM Special Publication No. 83, SEPM Society For Sedimentary Geology), 231–256, 2005.
Kroonenberg, S. B., Abdurakhmanov, G. M., Badyukova, E. N., van der Borg, K., Kalashnikov, A., Kasimov, N. S., Rychagov, G. I., Svitoch, A. A., Vonhof, H. B., and Wesselingh, F. P.: Solar-forced 2600 BP and Little Ice Age highstands of the Caspian Sea, Quatern. Int., 173–174, 137–143, 2007.
Lahijani, H. and Tavakoli, V.: Identifying provenance of South Caspian coastal sediments using mineral distribution pattern, Quatern. Int., 261, 128–137, 2012.
Lahijani, H. A. K., Tavakoli, V., and Amini, A. H.: South Caspian river mouth configuration under human impact and sea level fluctuations, Environ. Sci., 5, 65–86, 2008.

BGD
9, 16663–16704, 2012

Leroy, S. A. G.: Palaeoenvironmental and palaeoclimatic changes in the Caspian Sea region since the Lateglacial from palynological analyses of marine sediment cores, Geography, Environment, Sustainability, 2, 32–41, 2010.

Leroy, S. A. G., Lahijani, H. A. K., Djamali, M., Naqinezhad, A., Moghadam, M. V., Arpe, K., Shah-Hosseini, M., Hosseindoust, M., Miller, C. S., Tavakoli, V., Habibi, P., Naderi, M.: Late Little Ice Age palaeoenvironmental records from the Anzali and Amirkola lagoons (South Caspian Sea): vegetation and sea level changes, Palaeogeogr. Palaeocl., 302, 415–434, 2011.

Leroy, S. A. G., Marret, F., Giralt, S., and Bulatov, S. A.: Natural and anthropogenic rapid changes in the Kara-Bogaz Gol over the last two centuries by palynological analyses, Quatern. Int., 150, 52–70, 2006.

Leroy, S. A. G., Marret, F., Gibert, E., Chalié, F., Reyss, J.-L., and Arpe, K.: River inflow and salinity changes in the Caspian Sea during the last 5500 years, Quatern. Sci. Rev., 26, 3359–3383, 2007.

Lewis J. and Hallett R: *Lingulodinium polyedrum* (*Gonyaulax polyedra*) a blooming dinoflagellate, Oceanogr. Mar. Biol. Annu. Rev., 35, 97–161, 1997.

Loeblich, A. R. and Tappan, H.: Foraminiferal Genera and their Classification, Van Nostrand Reinhold, New York, 1182 pp., 1987.

Londeix, L., Herreyre, Y., Turon, J.-L., and Fletcher, W.: Last Glacial to Holocene hydrology of the Marmara Sea inferred from a dinoflagellate cyst record, Rev. Palaeobot. Palyno., 158, 52–71, 2009.

Makhlough, A., Nasrollahzadeh, H. S., Pourgholam, R., and Rahmati, R.: The Introduction of toxic and harmful new species of phytoplankton in the Iranian costal water of the Southern Caspian Sea, J. Biol. Sci. Lahijan, 5, 77–93, 2011 (in Persian).

Marret, F. and Zonneveld, K. A. F.: Atlas of modern organic-walled dinoflagellate cyst distribution, Rev. Palaeobot. Palyno., 125, 1–200, 2003.

Marret, F., Leroy, S., Chalié, F., and Gasse, F.: New organic-walled dinoflagellate cysts from recent sediments of Central Asian seas, Rev. Palaeobot. Palyno., 129, 1–20, 2004.

Marret, F., Mudie, P., Aksu, A., and Hiscott, R. N.: A Holocene dinocyst record of a two-step transformation of the Neoeuxinian brackish water lake into the Black Sea, Quatern. Int., 197, 72–86, 2009.

BGD

9, 16663–16704, 2012

McCarthy, F. M. G. and Mudie, P. J.: Oceanic pollen transport and pollen : dinocyst ratios as markers of late Cenozoic sea level change and sediment transport, Palaeogeogr., Palaeocl., 138, 187–206, 1998.

Mertens, K., Ribeiro, S., Bouimetarhan, I. et al.: Process length variation in cysts of a dinoflagellate, *Lingulodinium machaerophorum*, in surface sediments: investigating its potential as salinity proxy, Mar. Micropaleontol., 70, 54–69, 2009.

Mudie, P. J., Leroy, S. A. G., Marret, F., Gerasimenko, N., Kholeif, S. E. A., Sapelko, T., and Filipova-Marinova, M.: Non-Pollen Palynomorphs: Indicators of Salinity and Environmental Change in the Caspian-Black Sea-Mediterranean Corridor. in Geology and Geoarchaeology of the Black Sea Region: Beyond the Flood Hypothesis, edited by: Buynevich, I., Yanko-Hombach, V., Gilbert, A. S., and Martin, R. E., Geological Society of America Special Paper, 473, 89–115, 2011.

Nadirov, R. S., Bagirov, E., Tagiyev, M., and Lerche, I.: Flexural plate subsidence, sedimentation rates, and structural development of the super-deep South Caspian Basin, Mar. Petrol. Geol., 14, 383–400, 1997.

NASA: available at: http://data.giss.nasa.gov/gistemp/, last access: 30 August 2012.

Nasrollahzadeh, H. S., Din, Z. B., Foong, S. Y., and Makhlough, A.: Trophic status of the Iranian Caspian Sea based on water quality parameters and phytoplankton diversity, Cont. Shelf Res., 28, 1153–1165, 2008a.

Nasrollahzadeh, H. S., Din, Z. B., Foong, S. Y., and Makhlough, A.: Spatial and temporal distribution of macronutrients and phytoplankton before and after the invasion of the ctenophore, *Mnemiopsis leidyi*, in the Southern Caspian Sea, Chem. Ecol., 24, 233–246, 2008b.

Nasrollahzadeh, H. S., Maklough, A., Pourgholam, R., Vahedi, F., Qanqermeh, A., and Foong, S. Y.: The study of *Nodularia spumigena* bloom event in the Southern Caspian Sea, Appl. Ecol. Environ. Res., 9, 141–155, 2011.

Omrani Rekavandi, H., Sauer, E. W., Wilkinson, T., Safari Tamak, E., Ainslie, R., Mahmoudi, M., Griffiths, S., Ershadi, M., Jansen Van Rensburg, J., Fattah, M., Ratcliffe, J., Nokandeh, J., Nazifi, A., Thomas, R., Gale, R., and Hoffmann, B.: An Imperial frontier of the Sasanian Empire: further fieldwork at the great wall of Gorgan, Iran, 45, 95–136, 2007.

Patimar, R.: Fish species diversity in the lakes of Alma-Gol, Adji-Gol, and Ala-Gol, Golestan province, Northern Iran, J. Ichthyol., 48, 911–917, 2008.

BGD

9, 16663–16704, 2012

Patimar, R., Yousefi, M., and Hosieni, S. M.: Age, growth and reproduction of the sand smelt Atherina boyeri Risso, 1810 in the Gomishan wetland – Southeast Caspian Sea, Estuar. Coast. Shelf S., 81, 457–462, 2009.

Pierret, M. C., Chabaux, F., Leroy, S. A. G., and Causse, C.: A record of Late Quaternary continental weathering in the sediment of the Caspian Sea: evidence from U-Th, Sr isotopes, trace element and palynological data, Quatern. Sci. Rev., 51, 40–55, 2012.

Reyss, J.-L., Schmidt, S., Legeleux, F., and Bonte, P.: Large, low background well-type detectors for measurements of environmental radioactivity, Nucl. Instrum. Meth. A, 357, 391–397, 1995.

Schumacher, B. A.: Methods for the Determination of Total Organic Carbon (TOC) in Soils and Sediments, US Environmental Protection Agency, Las Vegas, NV, 2002.

Sgarrella, F. and Moncharmont Zei, M.: Benthic foraminifera of the Gulf of Naples (Italy): systematic and autoecology, Boll. Soc. Paleontol. I., 32, 145–264, 1993.

Soloviev, D.: Identification of the extent and causes of Cyanobacterial bloom in September–October 2005 and development of the capacity for observation and prediction of HAB in the Southern Caspian Sea using Remote Sensing Technique, available at: http://www.caspianenvironment.org/newsite/DocCenter/2006/HABrepFinalFull_corrected_compressed_pictures.doc, 2005, last access: 23 June 2012.

Tagiyev, M. F., Nadirov, R. S., Bagirov, E. B., and Lerche, I.: Geohistory, thermal history and hydrocarbon generation history of the North-west South Caspian basin, Mar. Petrol. Geol., 14, 363–382, 1997.

Tuzhilkin, V. S. and Kozarev, A. N.: in The Caspian Sea environment, edited by: Kostianoy, A. and Kosarev, A., Springer Berlin, Heidelberg, 33–57, 2005.

USDA: avaiable at: http://www.pecad.fas.usda.gov/cropexplorer/global_reservoir/gr_regional_chart.cfm?regionid=metu\&region=\&reservoir_name=Caspian, last access: 30 August 2012.

Verleye, T., Mertens, K. N., Louwye, S., and Arz, H. W.: Holocene Salinity changes in the Southwestern Black Sea: a reconstruction based on dinoflagellate cysts, Palynology, 33, 77–100, 2009.

Voronina, E., Polyak, L., de Vernal, A., and Peyron, O.: Holocene variations of sea-surface conditions in the Southeastern Barents Sea, reconstructed from dinoflagellate cyst assemblages, J. Quatern. Sci., 16, 7, 717–726, 2001.

BGD
9, 16663–16704, 2012

Voropayev, G. V., Kransnozhon, G. F., and Lahijani, H.: Riverine sediments and stability of Iranian coast of the Caspian Sea, Water Resour., 25, 747–758, 1998.
Zaker, N. H., Ghaffari, P., and Jamshidi, S.: Physical study of the southern coastal waters of the Caspian Sea, off Babolsar, Mazandaran, Iran, J. Coastal Res., 50, 564–569, 2007.
Zaker, N. H., Ghaffari, P., Jamshidi, S., and Nouranian, M.: Currents on the Southern Continental Shelf of the Caspian Sea off Babolsar, Mazandaran, Iran, J. Coastal Res., 64, 1989–1997, 2011.
Zenkevitch, L. A.: Biology of the Seas of the USSR, George Allen and Unwin Ltd, London, 1963.

BGD
9, 16663–16704, 2012

Table A1. Location of surface samples for dinocysts according to increasing values of *L. machaerophorum* B.[1]Kazancıet al. (2004); [2] Leroy et al. (2006). n/a: not available.

Label	lat N	long E	water depth in m	Location brief description	Sampling date	Type of sample	Surface temperature in C	Surface salinity	Date of measurements & source	Published palynological sample label
Almagol	37 25 53.50	54 38 52.18	0,6	core top in Modern Lagoon, water at zero	Sept. 2010	lagoon	11 - 28	2 - 3	not measured at sampling; Patimar (2008) for 2000-2002	
Alagol	37 21 59.48	54 34 44.33	0,6	core top in Modern Lagoon, water at -6 m	Sept. 2010	lagoon	10 - 27	3.5 - 4.0	not measured at sampling; Patimar (2008) for 2000-2002	
Anzali09	37 26 56.6	49 22 49.8	1,8	grab HCGA09, 280 m away	26 June 2008	lagoon	n/a	n/a	not measured at sampling	
Anzali 6	37 25 1.94	49 25 17.93	c. 1-2	grab Anzali Lagoon surface	1995	lagoon	4.5 - 27.5	0.8 - 3.0	not measured at sampling; but across 2000 [1]	Ens8 [1]
US24	43 19 14	49 06 02	61	core top	Aug. 1994	marine	25,5	9.5	F. Chalié, snapshot	
US02	39 16	51 28	315	core top, SR9406US14, SR01US9402, at 0.5 cm depth	Aug. 1994	marine	24,7	10.9	F. Chalié, snapshot	US02 [2]
Anzali 3	37 29 5.62	49 19 14.05	c. 1-2	grab Anzali Lagoon surface	1995	lagoon	4.5 - 27.5	0.5 - 4.5	not measured at sampling; but across 2000 [1]	Ens15 [1]
Anzali 100	37 36	49 32	100	grab for phytoplankton	Jan. 2011	marine	9.3 - 30	7 - 11	H. S. Nasrollahzadeh, annual	
Astara20 W	38 24	49 01	20	grab for phytoplankton	Winter 2010	marine	7.5 - 33	7.5 - 14	H. S. Nasrollahzadeh, annual	
Torkman20	37 05	53 35	20	grab for phytoplankton	Winer 2010	marine	? - 29.5	9 - 10	H. S. Nasrollahzadeh, annual	
US01	38 44 10	53 11 15	13	core top, SR9403US09, SR01US9401, at 0.5 cm depth	Aug. 1994	marine	28	10.5	F. Chalié, snapshot	
CS10	36 48 25.0	52 33 02.8	250	core top, core CS10 at 2cm	2007	marine	18	12	not measured at sampling, but snapshot for a station with 42 m water depth in Nov. 2008 (Jamshidi & BinAbuBakar 2011)	
Astara 100	38 22	49 08	100	grab for phytoplankton	Summer 2010	marine	7.8 - 32.4	7 - 12	H. S. Nasrollahzadeh, annual	
Astara 20S	38 24	49 01	20	grab for phytoplankton	Summer 2010	marine	7.5 - 32.6	7.5 - 14	H. S. Nasrollahzadeh, annual	
Babol100	36 49	52 39	100	grab for phytoplankton, babolsar	Jan. 2011	marine	9.6 - 28	9.5 - 13	H. S. Nasrollahzadeh, annual	
US26	43 19 36	49 05 58	61	core top	Aug. 1994	marine	25,5	9.5	F. Chalié, snapshot	
CS03	37° 35 28.3	49 34 16.6	250	core top, core CS03 at 2 cm	2007	marine	10	12	not measured at sampling, but for a station nearby in 2008 (Ghaffari et al. 2010; S. Haghani)	
Anzali 4	37 25 18.16	49 26 48.36	c. 1-2	grab Anzali Lagoon surface	1995	lagoon	4.5 - 27.5	1.0 - 5.0	not measured at sampling; but across 2000 [1]	Ens6 [1]
Anzali 20	37 30	49 29	20	grab for phytoplankton	Jan. 2011	marine	7 - 32	7 - 10	H. S. Nasrollahzadeh, annual	
Anzali 2	37 27 40.01	49 22 11.41	c. 1-2	grab Anzali Lagoon surface	1995	lagoon	4.5 - 27.5	0.5 - 1.0	not measured at sampling; but across 2000 [1]	Ens12 [1]
Babol20	36 46	52 40	20	grab for phytoplankton, Babolsar	Jan. 2011	marine	10 - 29.4	8 - 11.4	H. S. Nasrollahzadeh, annual	
Anzali 1	37 24 55.24	49 29 9.12	c. 1-2	grab Anzali Lagoon surface	1995	lagoon	4.5 - 27.5	0.6 - 2.0	not measured at sampling; but across 2000 [1]	Ens1 [1]
BTorkman 2	36 53 57.3	54 02 46.1	c. 0.1	artificial pool behind bay, salinity 22, reeds, *Salicornia*	20 May 2011	lagoon	n/a	**22**	S. Leroy, snapshot	
BTorkman 1	36 53 49.7	54 02 39.4	c. 0.1	harbour, salinity 17, mud with *Salicornia* meadow	20 May 2011	lagoon	n/a	**17**	S. Leroy, snapshot	
TR1	37 03 43.70	54 01 59.02	0,1	core top in Modern Lagoon, water at -28 m, Gm1short	Sept. 2010	lagoon	9 - 30	**20 - 24**	Spring-Summer in 2007 (Patimar et al. 2009)	
AS17	46 31 04	60 41 55	12,5	core top, AS17-5 at 0.5 cm	17 June 1999	marine	n/a	22	(Boomer et al. 2003; S. Juggins pers. comm.) snapshot	AS0.5 [2]
KBG08-01	41 51	53 15	0,8	core top, KBG08-01 at 0.5 cm depth	1999	marine	-3.5 - +33	170 - 250	1999 [2]	KBG08-01 [2]

BGD
9, 16663–16704, 2012

Table A2. Core numbering and location. Note: locations and water depths for the two Usnel cores are approximate owing to poor weather conditions and navigation tool performances.

Full name **General location**	Short name	Length (cm)	Latitude N Longitude E	Water depth (m)	Date Corer
On board no SR9403US09 Museum no SR01US9401 **Off shore Turkmenistan**	**US01**	36	38° 44′ 10″ 53° 11′ 15″	13	1994 Usnel box
On board no SR9406US14 Museum no SR01US9402 **Centre of south basin**	**US02**	57	39° 16′ 51° 28′	315	1994 Usnel box
CS07-03 **Off shore Anzali**	**CS03**	166	37° 35′ 28.3″ 49° 34′ 16.6″	250	2007 Piston
CS07-10 **Off shore Babolsar**	**CS10**	147	36° 48′ 25.0″ 52° 33′ 02.8″	250	2007 Piston

BGD
9, 16663–16704, 2012

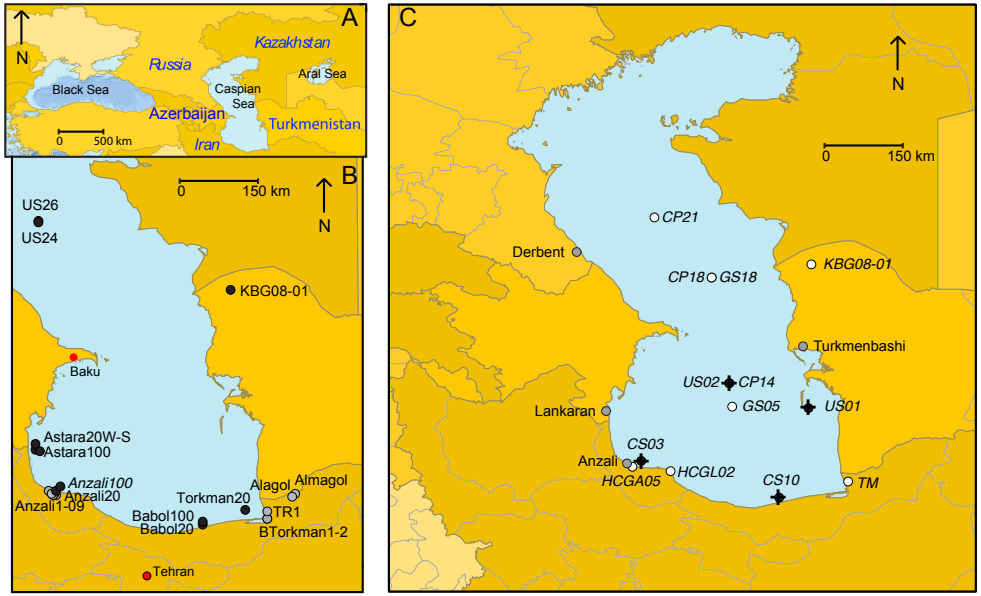

Fig. 1. Location maps. **(A)**: Location of the Caspian Sea at the boarder between Europe and Asia. **(B)**: Location of the surface samples in the Caspian Sea (black dots for marine samples and grey dots for lagoonal samples), and capital cities (red dots). **(C)**: Location of the four short cores (black dots with cross), the other Caspian cores (white dots) and the meteorological stations (gray dots).

BGD
9, 16663–16704, 2012

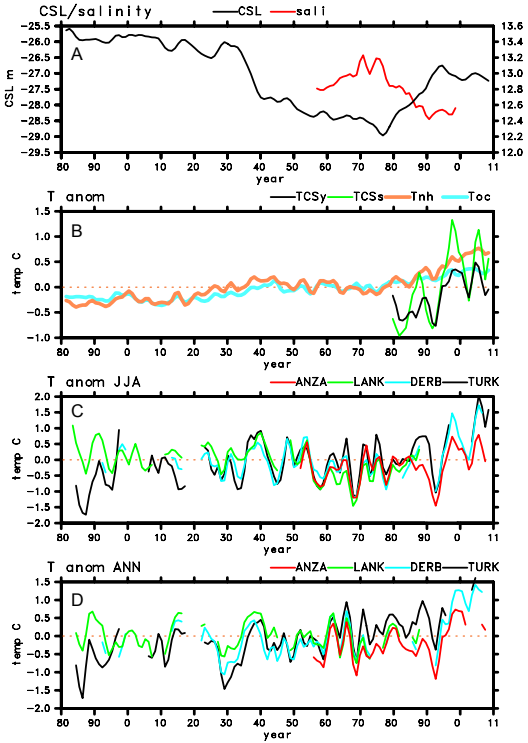

Fig. 2. Selected oceanographic and meteorological data for the Caspian Sea. All data are smoothed with a 1-2-1 filter. Anomalies are used for panels **(B)**, **(C)** and **(D)**. **(A)** Caspian Sea level (CSL) (Cazenave et al., 1997; Golitsyn and Panin, 1989; USDA, 2012) and summer surface salinity from the centre of the middle basin (sali) (Tuzhilkin and Kosarev, 2005). **(B)** sea surface temperatures of Southern Caspian Sea from analysis (TCSy = CS year-January–December; TCSs = CS summer-JJA.) (Dee et al., 2011); annual mean 2 m temperatures of the Northern Hemisphere (Tnh) and annual mean of global ocean temperatures (Toc) (NASA, 2012). **(C)** 2 m temperatures in summer (JJA) for the following meteorological stations (Climatic Research Unit, University of East Anglia, 2012): ANZA = 407 180, 37.5° N 49.5E, −26 m a.s.l., Anzali, Iran LANK = 379 850, 38.7° N 48.8° E, −12 m a.s.l., Lankaran, Azerbaijan DERB = 374 700, 42.0° N 48.3° E, −19 m a.s.l., Derbent, Russia TURK = 385 070, 40.1° N 53.0° E, 82 m a.s.l., Turkmenbashi, Turkmenistan **(D)** annual 2 m temperatures for stations in 2 °C (Climatic Research Unit, University of East Anglia, 2012).

BGD
9, 16663–16704, 2012

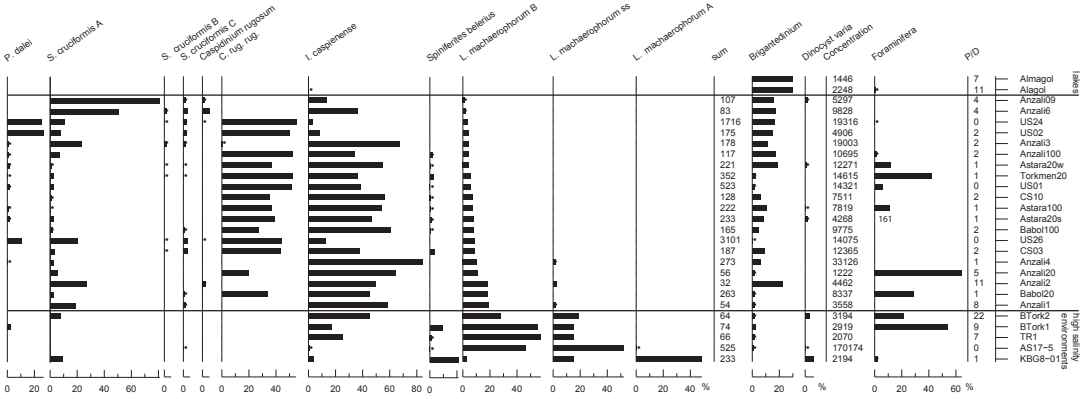

Fig. 3. Dinocyst assemblages from marine and lagoonal surface samples, mostly from the south basin of the Caspian Sea, topmost samples from two lakes and bottommost samples from high salinity environments. Percentages on sum of all dinocysts, except *Brigantedinium*. For the latter and for the foraminifera linings the sum also includes respectively *Brigantedinium* or foraminifera. Concentration in numbers of dinocysts ml^{-1} of wet sediment.

BGD
9, 16663–16704, 2012

***Lingulodinium machaerophorum* expansion in the Caspian Sea**

S. A. G. Leroy et al.

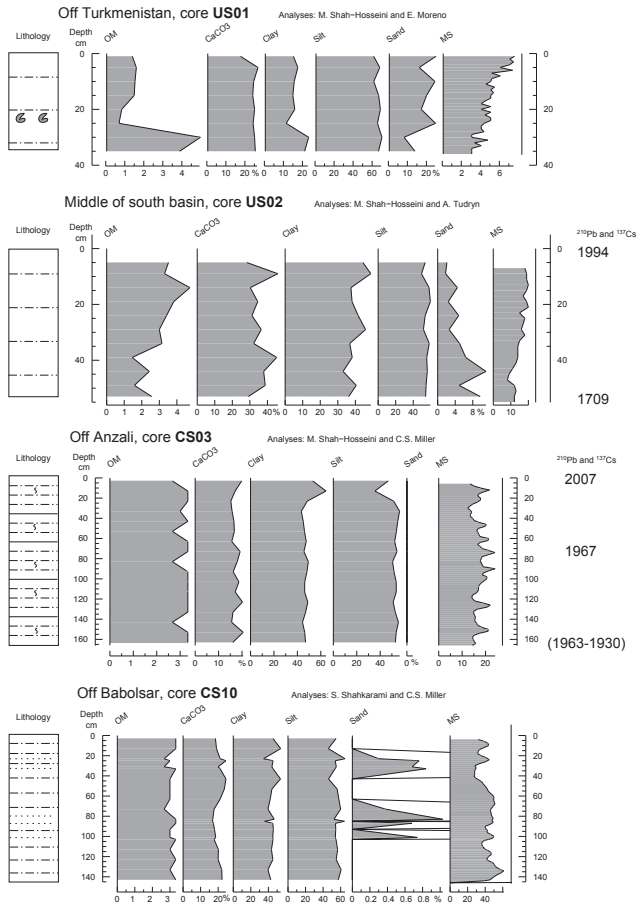

Fig. 4. Sedimentology of the four short cores: visual description of the lithology, organic matter (OM) and calcium carbonate ($CaCO_3$) contents in percentages after Loss-On-Ignition, clay, silt and sand percentages by particle size analysis, as well as magnetic susceptibility (MS).

BGD
9, 16663–16704, 2012

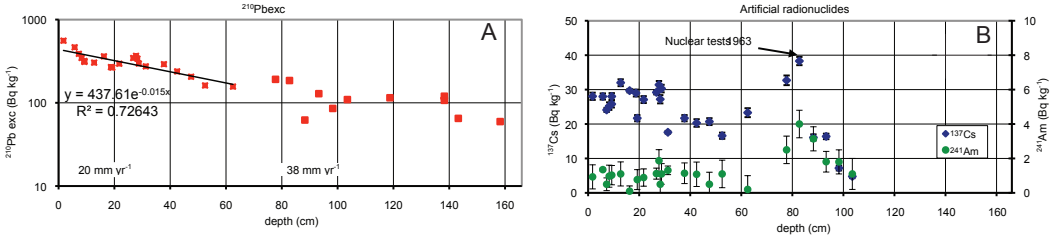

Fig. 5. Radionuclide dating of core CS03. **(A)** Profiles of ^{210}Pbexc. Activities (Bq kg^{-1}, dry weight) with depth in cm. The regression line between the top and 65 cm depth corresponds to an average sedimentation rate of 2.0 cm yr^{-1}. Deeper in the core the regression line corresponds to 3.8 cm yr^{-1}. **(B)** Profiles of artificial radionuclides ^{137}Cs and ^{241}Am activities (fallout from nuclear weapon testing) with depth in cm. The maximum activity at 83 cm depth for both nuclides corresponds to the maximum global fallout peak in 1963.

BGD
9, 16663–16704, 2012

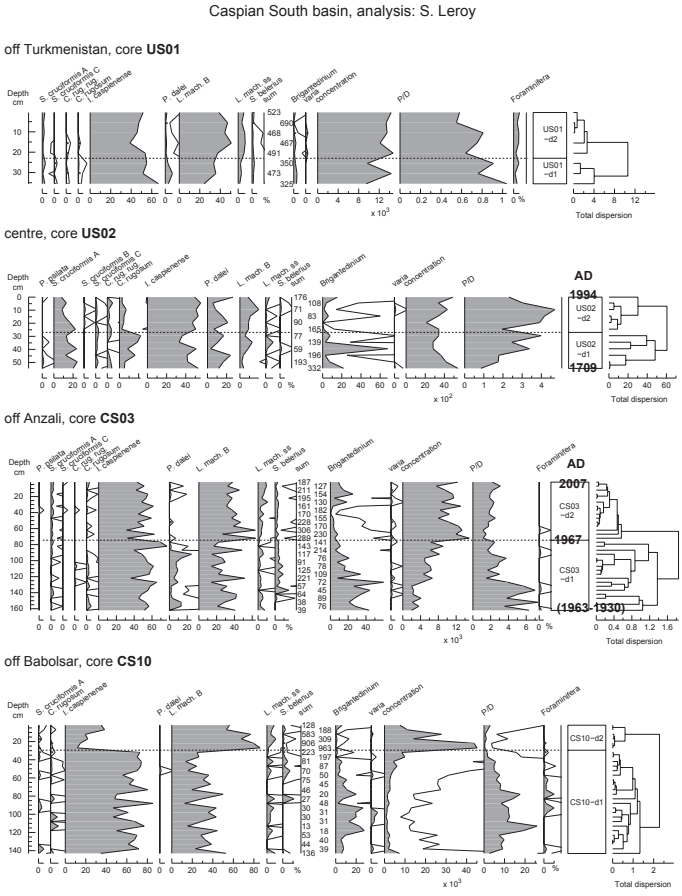

Fig. 6. Dinocyst diagrams of cores US01, US02, CS03 and CS10, taken in the south basin of the Caspian Sea. Concentration in numbers of dinocysts ml^{-1} of wet sediment. With 10× exaggeration curve. To the right dendrograms used for the zonation.

BGD
9, 16663–16704, 2012

***Lingulodinium machaerophorum* expansion in the Caspian Sea**

S. A. G. Leroy et al.

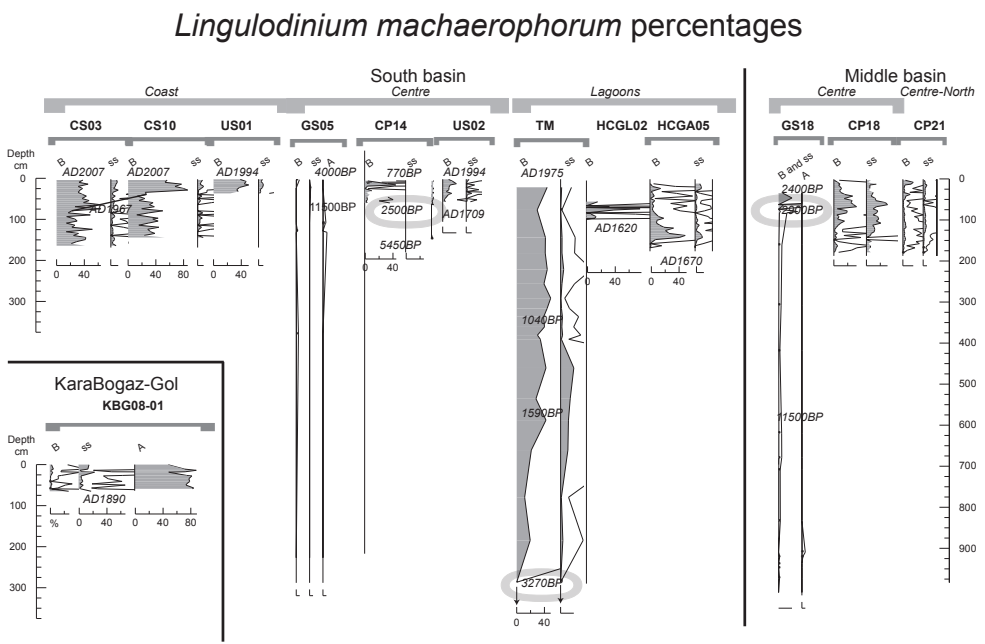

Fig. 7. The three forms of *Lingulodinium machaerophorum* in thirteen cores of the Caspian Sea over the last few millennia. The three grey ovals underline the start of the *L. machaerophorum* development. Black dots for values lower than 0.5 %. The percentages were calculated for sums excluding *Brigantedinium*. Core KBG08 (Leroy et al., 2006); cores GS05 and GS18 (Leroy, personal communication, 2012); part of core TM (Kakroodi et al., 2012); cores HCGL02 and HCGA05 (Leroy et al., 2011); cores CP14, CP18 and CP21 (Leroy et al., 2007). The grey circles indicate the start of the *L. machaerophorum* development. B, ss and A are the three forms of *L. machaerophorum*. Dates in AD or in calibrated years BP. With 10× exaggeration curve.

BGD
9, 16663–16704, 2012

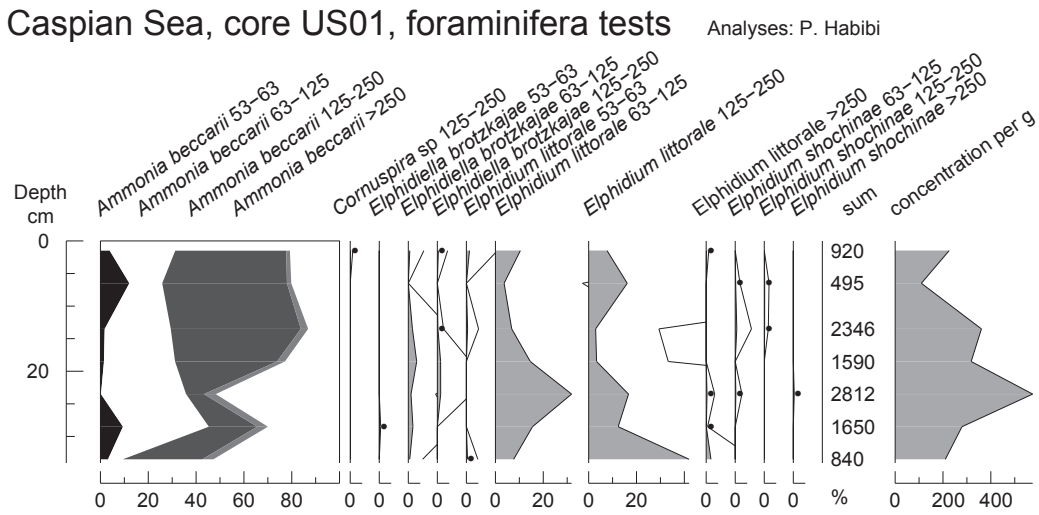

Fig. A1. Foraminifera assemblages of core US01, taken in the south basin of the Caspian Sea. Names with fraction size in µm.

BGD
9, 16663–16704, 2012

***Lingulodinium machaerophorum* expansion in the Caspian Sea**

S. A. G. Leroy et al.